Battarra *et al. Biology Direct* (2024) 19:108
https://doi.org/10.1186/s13062-024-00545-3

Biology Direct

RESEARCH Open Access

Efficient DNA-free co-targeting of nuclear genes in *Chlamydomonas reinhardtii*

Claudia Battarra[1], Max Angstenberger[1,2*], Roberto Bassi[1*] and Luca Dall'Osto[1]

Abstract

Chlamydomonas reinhardtii, a model organism for unicellular green microalgae, is widely used in basic and applied research. Nonetheless, proceeding towards synthetic biology requires a full set of manipulation techniques for inserting, removing, or editing genes. Despite recent advancements in CRISPR/Cas9, still significant limitations in producing gene knock-outs are standing, including (i) unsatisfactory genome editing (GE) efficiency and (ii) uncontrolled DNA random insertion of antibiotic resistance markers. Thus, obtaining efficient gene targeting without using marker genes is instrumental in developing a pipeline for efficient engineering of strains for biotechnological applications. We developed an efficient DNA-free gene disruption strategy, relying on phenotypical identification of mutants, to (i) precisely determine its efficiency compared to marker-relying approaches and (ii) establish a new DNA-free editing tool. This study found that classical CRISPR Cas9-based GE for gene disruption in *Chlamydomonas reinhardtii* is mainly limited by DNA integration. With respect to previous results achieved on synchronized cell populations, we succeeded in increasing the GE efficiency of single gene targeting by about 200 times and up to 270 times by applying phosphate starvation. Moreover, we determined the efficiency of multiplex simultaneous gene disruption by using an additional gene target whose knock-out did not lead to a visible phenotype, achieving a co-targeting efficiency of 22%. These results expand the toolset of GE techniques and, additionally, lead the way to future strategies to generate complex genotypes or to functionally investigate gene families. Furthermore, the approach provides new perspectives on how GE can be applied to (non-) model microalgae species, targeting groups of candidate genes of high interest for basic research and biotechnological applications.

Keywords *Chlamydomonas reinhardtii*, Microalgae, Genome editing, CRISPR/Cas9, Nonhomologous end joining, Antibiotic-free

*Correspondence:
Max Angstenberger
m.angstenberger@bio.uni-frankfurt.de
Roberto Bassi
roberto.bassi@univr.it
[1]Department of Biotechnology, University of Verona, Cà Vignal 1, Strada le Grazie 15, 31734 Verona, Italy
[2]Institute of Molecular Biosciences, Goethe University Frankfurt am Main, Max-von-Laue-Str.9, 60438 Frankfurt am Main, Germany

Introduction

The unicellular green microalga *Chlamydomonas reinhardtii* (*C. r.*) is a well-established model organism for basic and applied research due to its potential as a cell factory for the sustainable production of a wide range of recombinant proteins and metabolites [1–3]. The fully sequenced genome allows the investigation of specific gene functions and the pursuit of advanced biotechnological applications. Several strategies have been developed to knock-out (KO) or knock-down genes, including chemical, physical, and insertional mutagenesis. RNA-based approaches such as RNA interference (RNAi) or artificial microRNAs (amiRNA) [4] are still facing limitations such as low editing efficiency, non-specific targeting, or even silencing of inserted constructs [5, 6]. Thus, targeted gene disruption strategies represent the major nuclear genome-editing (GE) tools available, including zinc finger nucleases (ZFNs), transcriptional activator-like effector nucleases (TALENs), and, especially, clustered regularly interspaced short palindromic repeats (CRISPR)/Cas9 nuclease system [7].

TALENs- and ZFNs-dependent gene disruption suffers for several adverse side effects, such as a high off-target mutation frequency and time-consuming laboratory procedures to produce new targets [8]. In contrast, the CRISPR/Cas9 system is cheap and time-efficient [9, 10], yielding precise and targeted genetic manipulations. Further improvement of efficiency and specificity is essential for creating easy-to-detect phenotypes that can be used as an alternative to selectable markers for antibiotic-free GE in transformation approaches towards multiple targets, substituting for the need for DNA integration.

In principle, CRISPR-Cas9 technology for targeted gene disruption relies on the specific nuclease activity of CRISPR-associated protein 9 (Cas9) and its assembly with a single guide RNA (sgRNA), which is mainly constituted of two components: (i) the CRISPR RNA or crRNA, which is made of a 20 base pairs oligo sequence complementary to the target sequence, and (ii) a trans-activating CRISPR RNA (tracrRNA) [11]. Cas9-sgRNA complex specifically binds the target genomic DNA sequence. It generates a DNA double-stranded break (DSB), which can be repaired by two main mechanisms: by the error-prone and DNA template independent non-homologous end joining (NHEJ), often resulting in minor false DSB repair or by the homology-directed repair (HDR) pathway [12, 13] depending on the presence of homologous sequences in a provided DNA repair template. Importantly, functional gene disruption upon applying GE approaches must always be verified due to undesired DSB repair events resulting in still (partially) functional gene versions, making intensive screening steps necessary to identify desired mutants. Recent approaches for further optimization of the CRISPR/Cas system applied to *C. r.* have been implemented in different ways: (i) as a transgenic system in which the components are expressed either transiently [7, 14, 15] or stably [13, 16]; (ii) as a transgene-free approach, by pre-assembling Cas9 proteins and sgRNA into ribonucleoprotein (RNPs) complexes then delivered into the cells by electroporation [6, 13, 15, 17–20] or (iii) by using a cell penetrating peptide [21].

However, DNA-based GE approaches of *C. r.* still need to overcome several challenges, such as genomic positioning effects based on NHEJ-mediated random insertion of foreign DNA, which might result in genomic rearrangements accompanied by the need for antibiotic selection, also occurring in more unspecific approaches as in random insertional mutagenesis. Moreover, approaches exploiting the transient expression of Cas9 can lead to severe immune responses and cellular toxicity [22, 23]. Avoiding DNA insertion for targeted gene disruption by exploiting RNPs in *C. r.* [17] turned out an elegant solution to overcome the mentioned side effects. Thus, it was further investigated to improve efficiencies and to establish effective multiple gene targeting.

Hence, focussing on reported efficiencies of various GE strategies in *C. r.*, we found some significant bottlenecks hampered clear interpretation and comparison: (i) a wide range of reported GE efficiencies [20]; (ii) undefined optimal cell cycle stages for transformation; (iii) usage of different *C. r.* strains, type of nuclease, target genes, repair templates (donor-DNA), and transformation methods [24]; (iv) availability and application of selective markers [25]; (v) limitation by positioning effects [20]; (vi) requirement of an optimal ratio of sgRNA and Cas protein [13, 25] and (vii) application of pre-selection [24]. In addition, KO frequencies are dependent on the number of electroporated cells [6, 13, 17, 19, 26]. Thus, statistically relevant data describing the differences between GE efficiencies upon application of antibiotic markers vs. strategies not introducing foreign DNA into cells (DNA-free approaches) has yet to be reported. A central aspect of this study was identifying the limiting step between Cas9-mediated DSB leading to gene KO and functional integration and expression of an antibiotic resistance marker in the genome. To this aim, all DNA-free GE approaches of this study were performed as methodologically close as possible to recent work [13], in which KO of the *CpFTSY* gene was obtained with a combination of RNP and either NHEJ or HDR-based DNA integration with further antibiotic selection. The central aspect of this GE strategy in *C.r.* was the exploitation of cultures synchronized at the same cell cycle stage, which dramatically increased GE efficiency [13]. The rapid identification of proper *cpftsy* KO lines of *C. r.* relies on the visible pale-green phenotype of colonies since the CpFTSY protein is involved in transporting and assembling light-harvesting

proteins into the thylakoid membranes [17]. Notably, obtaining *cpftsy* KO mutants was dependent on two events necessary to occur at the same time in the cell: (i) the introduction of a DSB by Cas9 for *CpFTSY* disruption and (ii) the functional integration and expression of the antibiotic resistance marker gene. A similar enhancement in GE efficiency was recently achieved [24] on *C. r.* cultures under nitrogen starvation, which forced cells to rest in the G_0-stage of the cell cycle before applying GE approaches.

To extend the possibilities of cell synchronization and confirm the effect, we tested phosphate starvation before gene disruption experiments.

Finally, PSR1, a transcriptional factor that modulates phosphate starvation response and is up-regulated during P deprivation [27], was selected for co-targeting experiments: a *psr1* KO mutant is unable to synthesize extracellular phosphatase in response to Pi deprivation, allowing easy confirmation of co-edited colonies through a colorimetric method. *PSR1*/*CpFTSY* co-editing experiments were performed to understand the potential of DNA-free multiplex GE towards genes lacking a selectable phenotype. Such a strategy could help to overcome constraints on the availability of antibiotic resistance markers and provide transgene-free *C. r.* strains for basic research and biotechnology.

Materials and methods

Gene identity and *C. reinhardtii* cultivation

Phytozome database (https://phytozome.jgi.doe.gov) was used to assess *Chlamydomonas reinhardtii* gene identity. Sequence data from this article can be found under accession entry Cre05.g241450 (*CpFTSY*) and Cre12.g495100 (*PSR1*). *C. reinhardtii* cell wall-deficient strain CW15 (CC-4533, chlamylibrary.org) was cultivated in either 20 mL flasks or 2 mL multi-well plates containing tris-acetate phosphate (TAP)-medium [28] or tris-acetate (TA)-medium lacking phosphate, both supplemented with 100 µg/mL of ampicillin and maintained at 25 °C under continuous white light at low intensity (50 µmol photons m^{-2} s^{-1}). Cultures were grown under light/dark and warm/cool cycles to promote cell cycle synchronization: 200 photons m^{-2} s^{-1} of white light, 28 °C for 12 h, and 12 h of darkness at 18 °C. Before the transformation, sub-culturing was carried out for two weeks under these conditions. Cells were grown in TAP medium up to full exponential growth phase to promote phosphate starvation, then harvested and resuspended in TA medium. Cells were grown in TA for 3 days to reach full phosphate starvation. Data in all experiments indicate the mean average and standard deviation (SD) from three ($n=3$) or six ($n=6$) biological replicates. Cell number was determined using a Countess II FL cell counter (Life Technologies) and a calibration factor of 2.

Genomic DNA isolation

Genomic DNA purification from *C. reinhardtii* CW15 was performed on 50 ml cultures from the early stationary phase, harvested at 12,000 x g for 30 s. Subsequently, cells were resuspended in 500–700 µL 2x CTAB buffer [29] supplemented with 100 µg Proteinase K and 50 µg RNAseA and incubated overnight at 60 °C on a rotator mixer. Genomic DNA was extracted using 1 unit of chloroform/isoamyl alcohol (24:1) after centrifugation at 12,000 x g for 30 s. This step was repeated with 1 unit of phenol (10 mM Tris-HCl pH 8.0) /chloroform/isoamyl alcohol (25:25:1) and 1 unit of chloroform. Finally, the extracted aqueous phase was mixed with 0.1 units of 0.3 M sodium acetate pH 5.0 and 1 unit of isopropanol. Nucleic acid precipitation was carried out at -20 °C for 30 min followed by centrifugation at 12,000 x g for 10 min. The sediment was washed twice with 70% ethanol (12,000 x g, 5 min) and dried for 1 h at 42 °C. Nucleic acids were resuspended in 30 µL 10 mM Tris-HCL pH 8.0. Isolation of in vitro transcribed sgRNA was carried out following the same protocol described for genomic DNA with minor changes: the starting volume has risen to 1 mL with diethyl pyrocarbonate (DEPC)-H_2O and phenol (10 mM Tris-HCl pH 5.0)/chloroform/isoamyl alcohol (25:25:1). The sediment was resuspended in 50 µL of DEPC-H_2O. Finally, the concentration of nucleic acids was determined using Nanodrop One (Thermo Scientific).

C. reinhardtii transformation

Transformation of the *C. reinhardtii* CW15 strain was performed as previously described [13] on 10^6 synchronized cells, harvested 4 h after lights-on. Cells were counted and harvested at 8,000 x g, 10 min at 15 °C and resuspended in 50 µL of TOS-Medium (80% v/v TAP, 40 mM sucrose). Before transformation, 6 µg of purified his-tagged Cas9 and 21.6 µg of sgRNA (composed of a 1:1 mix sgRNA, 50% target 1 (T1) *CpFTSY* and 50% trget 2 (T2) *CpFTSY*, see Fig. 1C) were pre-assembled in cleavage buffer (20 mM Tris-HCl pH 7.5, 20 mM KCl, 5 mM $MgCl_2$) for 30 min at 37 °C. The sgRNA sample in co-editing experiments included the 4 sgRNA in equimolar mixture (25% of each T1 *CpFTSY* / T2 *CpFTSY* / T1 *PSR1* / T2 *PSR1*). Subsequently, RNP complexes were added to the cell suspension and incubated for 5 min in darkness and on ice. The transformation was carried out in electroporation cuvettes 0.4 cm gap by a Gene Pulser II (Bio-Rad) set to 200 Ω, 50 µF, 0.6 kV. Recovery was achieved in 1.5 mL TOS-Medium, kept in darkness overnight on a rotator mixer. Cells were then counted and diluted to take 10 aliquots of 100 cells each. Finally, cells were resuspended in 500 µL of TAP-Medium containing 30% starch and plated on 1.5% Agar-TAP plates before incubation.

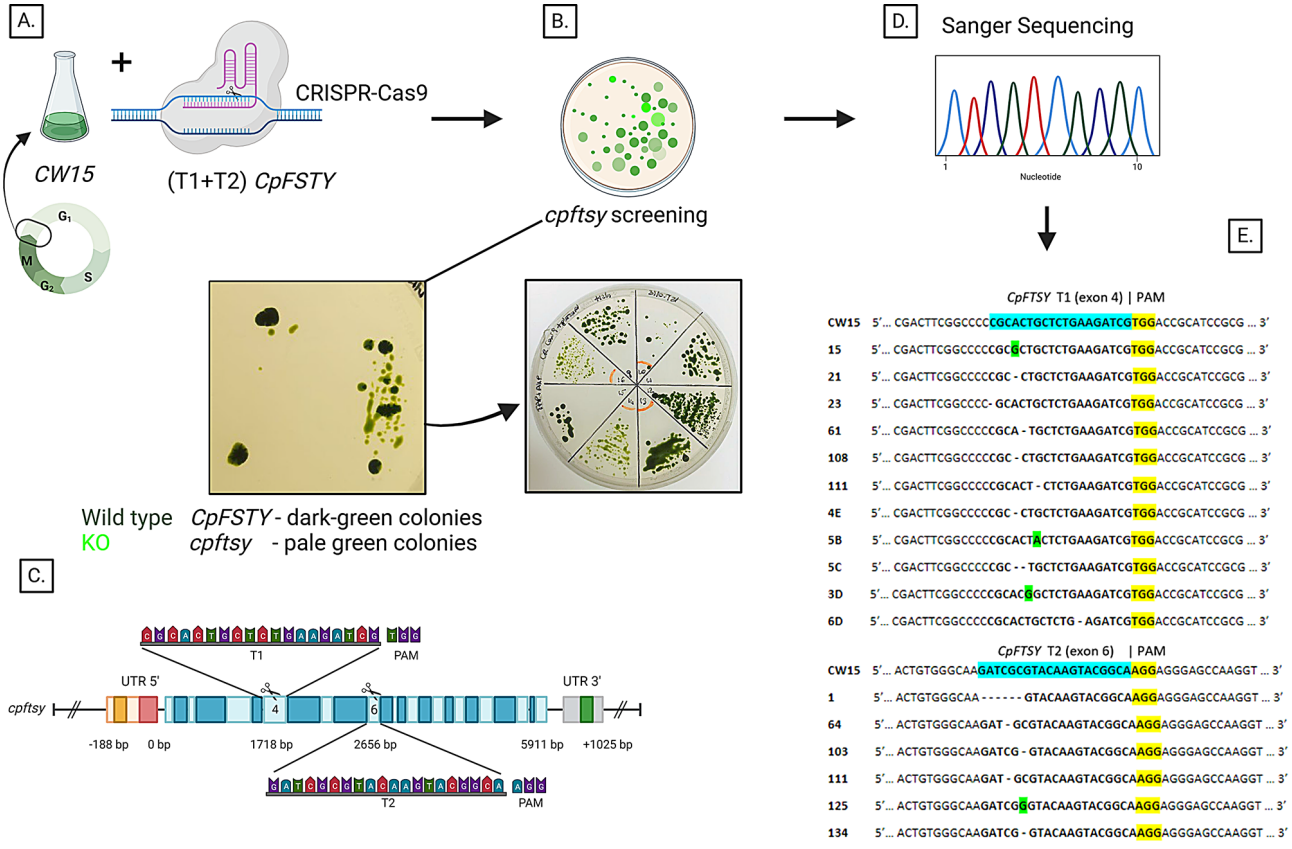

Fig. 1 DNA-free RNP-mediated GE strategy applied to *C. r.*CW15. (**A**) CW15 synchronized cells were transformed by electroporation with RNPs (assembled with Cas9, T1, and T2) to target the sequence of *CpFTSY*. (**B**) Transformed cells were plated on TAP agar plates, and potential KO cells were selected based on their pale-green phenotype. Then, colonies were streaked on new TAP agar plates to obtain individual and clean mutant lines. (**C**) Schematic CRISPR sgRNA design for knocking-out *CpFTSY* gene PAM sequences are shown. T1 and T2 are in exons 4 and 6, at position 1718 bp and 2656 bp, respectively (Fig. 1S, Table 1S). (**D**) Individual mutants were grown in liquid culture; PCR and Sanger sequencing were carried out after DNA extraction to pinpoint Cas9-induced mutations. (**E**) Sequencing data output of 17 pale-green colonies, showing the two target regions T1 and T2. Wild type sequences are highlighted in blue, Cas9 specific PAM motif in yellow. Missing nucleotides are indicated as "-", nucleotide substitutions are highlighted in green

sgRNA design and purification

The oligonucleotides (see Table 1S) sg_CP_fw1 and T7_CP_fw1 (target 1, T1) and sg_CP_fw2 and T7_CP_fw2 (target 2, T2) were used for *CpFTSY* sgRNA production, through in vitro transcription and purification, as previously described [13]. The same procedure was applied for *PSR1* sgRNA production, with oligonucleotides Psr1_fw and T7_Psr1_fw1 (target 1, T1), sg_Psr1_fw2 and T7_Psr1_fw2 (target 2, T2). The oligonucleotides were designed using www.e-crisp.org (access on 2019 and 2020, for *CpFTSY* and *PSR1* genes, respectively).

Mutant selection and characterization

The mutant screening was performed by growing cells in low density on 1.5% TAP-agar plates, supplemented with 30% starch, for about two weeks. Colonies exhibiting a pale-green phenotype were individually streaked on new 1.5% TAP-agar plates and subsequently cultivated in either 3 ml multi-well plates or 50 ml flasks. Cultures reached the stationary phase after about 15 days, after which genomic DNA was extracted. Co-targeting experiments were carried out by streaking pale-green colonies on TAP medium as mentioned above, then single drop spots of about 10 µl were put on 1.5% TA-agar plates. After 3 days of applied phosphate starvation, plates were sprayed with 10 mM 5-bromo-4-chloro-3-indolyl-P (X-Pi; Sigma-Aldrich, St. Louis) aqueous solution, a colorimetric substrate which turns blue after phosphate gets cleaved by secreted alkaline phosphatase. Plates were allowed to develop for 2 h before recording the results.

Amplification and sequencing

The precise editing was confirmed by sequencing of fragments amplified from genomic DNA. The PCR analysis was carried out using oligonucleotides CP_fw and CP_rv (see Table 2 S and Fig. 1S S) for amplification of both *CpFTSY* T1 and T2 (1.1 kb), primers PS_T1_fw and PS_T1_rv for *PSR1* T1 amplification (253 bp), PS_T2_fw and PS_T2_rv for *PSR1* T2 amplification (300 bp) (see Table 2 S and Fig. 3S, 4 S). Hybrid polymerase (EURX)

Table 1 Evaluation of the GE efficiencies (Y_{GE})

Experiment	Target	N_{CFU}	$N_{viable\ cells}$	$N_{pale\text{-}green\ colonies}$	$\%F_{GE\ CpFTSY}$	Precise edited colonies	T1 *CpFTSY*	T2 *CpFTSY*	T1 + T2 *CpFTSY*	$N_{pale\text{-}green\ colonies} \cdot D$	Y_{GE}	Ratio $_{GE\ efficiencies}$	± nt	⇄ nt
+P	*CpFTSY*	474 ± 63	1.02 ± 0.13 (· 10^5)	2.83 ± 0.75	0.61 ± 0.21	17/17	11/17	6/17	1/17	606 ± 161	6.06 ± 1.61 (· 10^{-4}) §,#	202 ± 53	76%	24%
-P	*CpFTSY*	527 ± 57	9.22 ± 1.01 (· 10^4)	4.67 ± 1.36	0.91 ± 0.32	22/28	14/22	8/22	2/22	817 ± 239	8.17 ± 2.39 (· 10^{-4}) §,#	272 ± 80	82%	18%

Experiment	Targets	N_{CFU}	$N_{viable\ cells}$	$N_{pale\text{-}green\ colonies}$	$\%F_{GE\ CpFTSY}$	Precise edited colonies	T1 *CpFTSY*	T2 *CpFTSY*	T1 + T2 *CpFTSY*	$N_{pale\text{-}green\ colonies} \cdot D$	Y_{GE}	Ratio $_{GE\ efficiencies}$	± nt	⇄ nt
Co-editing	*CpFTSY PSR1*	492 ± 51	1.05 ± 0.11 (· 10^5)	1.50 ± 0.55	0.30 ± 0.11	9/9	7/9	2/9	0/9	321 ± 117	3.21 ± 1.17 (· 10^{-4}) #	107 ± 39	100%	0%

$\%F_{GE\ CpFTSY\ \&\ PSR1}$	Precise co-edited colonies	T1 PSR1	T2 *PSR1*	T1 + T2 *PSR1*	$N_{pale\text{-}green\ \&\ no\text{-}halo\ colonies} \cdot D$	Y_{GE} (co-edit)	Ratio $_{GE\ efficiencies}$	± nt	⇄ nt
0.22 ± 0.11	2/9	1/9	1/9	0/9	71 ± 26	7.13 ± 2.60 (· 10^{-5}) #	24 ± 9	100%	0%

was applied to amplify the genes of interest. A reaction buffer (10 mM Tris-HCl pH 8.3, 50 mM KCl, 4 mM $MgCl_2$) was used for GC-rich sequence amplification. Reactions also contained 10 pmol of each primer, 0.53 mM dNTPs (each) and 0.26 M Betain. Annealing temperatures were 2−5 degrees below the supplier's reported melting temperature of primers, elongation to 30 s/kb at 72 °C. Amplification of template DNA and in vitro transcription of sgRNA were performed as reported [13]. The PCR products were purified (NucleoSpin, Gel and PCR clean-up kit) and sent for sanger sequencing (www.eurofinsgenomics.eu) and precise GE validation.

Calculation of the GE frequency

Formulas used for calculations are shown below, while raw data collected are reported in Table 3 S and 4 S. Formula abbreviations: N=number; F=frequency; Y, efficiency; R=replica; D=dilution factor.

The total number of CFU (colony forming units) was established by counting the number (N) of colonies for each transformation replica (R1 to R6):

$$N_{CFU} = N_{R1} + N_{R2} + N_{R3} + N_{R4} + N_{R5} + N_{R6}.$$

Then normalizing to the dilution factor (D), since aliquots were plated at 200-fold dilution on TAP Medium:

$$N_{viable\ cells} = N_{CFU} \cdot D.$$

The GE frequency (F_{GE}) was calculated by counting the number of pale-green colonies ($N_{pale-green\ colonies}$) over N_{CFU}:

$$F_{GE} = N_{pale-green\ colonies} / N_{CFU}.$$

The GE efficiency (Y_{GE}) was calculated by normalizing $N_{pale-green\ colonies}$ over $N_{viable\ cells}$, and considering the whole cell population (10^6 cells) which underwent electroporation:

$$Y_{GE} = N_{pale-green\ colonies} \cdot D / 10^6.$$

The ratio of GE efficiencies without (-AB, this study) and with antibiotic selection (+AB [13]), was calculated by the corresponding genome-editing efficiency:

$$Ratio_{GE\ efficiencies} = Y_{GE\ (-AB)} / Y_{GE\ (+AB)}.$$

Results

DNA-free GE strategy targeting *CpFTSY* in *Chlamydomonas reinhardtii*

To investigate factors that can enhance GE frequencies, we first implemented a DNA-free (i.e., antibiotic resistance marker-free) GE approach using RNP-mediated gene KO in *C. r.* by targeting the *CpFTSY* gene (Fig. 1), which is involved in the transport and assembly of light-harvesting proteins (LHC) into the thylakoid membranes [17, 20]. The parameters of the GE assay were optimized stepwise while using the standardized set of conditions [13] as a control.

Cultures of *C. r.* strain CW15 CC-4533 were synchronized by a specific light and temperature regime (Fig. 1A), transformed by electroporation using RNPs only, plated at low density to identify paler colonies, and then cleaned up by streaking selected colonies (Fig. 1B). Transformations were performed with many replicates to ensure statistically significant results ($n=6$). Two different sgRNAs (Fig. 1C), guiding the RNPs towards two specific target regions, were chosen for disrupting the *CpFTSY* gene, and then randomly selected pale-green colonies were analyzed by Sanger sequencing of the corresponding *CpFTSY* target sequence products (Fig. 1D and E).

In this context, GE frequency (% F_{GE}) was defined as the percentage of transformants showing a functional KO of the target gene due to either HR or NHEJ. Therefore, out of 17 pale-green lines we identified by PCR and sequencing screening (see Table 2 S and Figs. 3S and 4S),

frameshift mutations in 13 lines, which led to a functional loss of CpFTSY, while the remaining 4 lines exhibited single base substitutions, which however needed further analysis to confirm functional *CpFTSY* gene disruption. As expected, in most cases *CpFTSY* disruption was NHEJ-mediated, which resulted in a few base changes or deletions in either T1 (64.7% of selected lines) or T2 (35.3% of selected lines), mainly causing frameshifts for both T1 and T2. Nucleotide substitutions occurred with low frequency (27.3% for T1 and 16.7% for T2). Interestingly, we identified only one line (line 111) carrying frameshift mutations on both T1 and T2 (Fig. 4S). The % F_{GE}, calculated by the number of pale-green over total colonies, was 0.61±0.21 (n=6) (for comparison, see Tables 1 and 3S). By normalizing the number of pale-green colonies to the viable cells ($N_{viable\ cells}$, see Methods), a total number of 606±161 pale-green colonies would have been expected over the whole transformation sample (10^6 cells), resulting in a Y_{GE} of 6.06±161 ($\cdot 10^{-4}$).

Effect of phosphorus starvation on DNA-free GE efficiency

We further investigated the role of phosphorus (P) limitation, in the form of phosphate, on the GE efficiency, by forcing the G_0 phase of the cells [13, 24]. To this end, P was removed from the medium (Fig. 5S), and the growth of the culture was monitored over time. We found that a starvation time of at least 48 h was required to stop *C. r.* growth and arrest cell cycle in the G_0 phase. Therefore, P was removed from the pre-culture 72 h before transformation, which was carried out with the DNA-free methodology as described above (Fig. 1), by targeting the *CpFTSY* gene. The transformation resulted in an $\%F_{GE}$ of 0.91±0.32 (Table 1). It comes that P starvation, in combination with a DNA-free transformation, led to a Y_{GE} of 8.17±2.39 ($\cdot 10^{-4}$) [13]. Sequencing of the amplification products of the targeted *CpFTSY* exons confirmed that 22 out of 28 pale-green colonies were precisely edited at the target sites (Fig. 6S), with 14 lines edited in T1 (63.6% of selected lines) and 8 edited in T2 (36.3% of selected lines). Gene KOs were mainly caused by nucleotide deletion, while only 14.3% (in T1) and 25.0% (in T2) of lines showed a nucleotide substitution. Here, two selected colonies (lines P8 and P11) were simultaneously edited in both T1 and T2.

DNA-free co-targeting of *CpFTSY* and *PSR1*

To develop an innovative DNA-free tool not only for single gene editing, but also for co-editing multiple targets, we selected 2 targets. The first is the *CpFTSY* gene [17], which selective KO is expected to confer (i) an easy-selectable phenotype that can be used in the first selection round and (ii) an improved yield and better stress resistance under specific growth conditions [30] and, the second is the *PSR1* gene (Fig. 2A), encoding for a transcriptional factor downregulating the expression of alkaline phosphatase under P starvation, was chosen as the second GE target because (i) its disruption does not lead to a visible trait of the colonies and, therefore, can simulate whichever gene missing a detectable phenotype, and (ii) it can be easily screened by a colorimetric assay, following the pre-selection for *cpftsy* KO lines (Fig. 2). Indeed, upon targeting *PSR1*, a colorimetric assay using 5-bromo-4-chloro-3-indolyl phosphate (BCIP) was carried out to verify functional *PSR1* KOs, i.e., the loss of the ability of *C. r.* cells to accomplish the colorimetric reaction (Fig. 2B and C). Selected mutants were analyzed by Sanger sequencing of the corresponding CpFTSY (Fig. 1C) and PSR1 (Fig. 2E) target sequence PCR amplicons (Figs. 7, 8 and 9, 10 S).

In summary, we successfully isolated several pale-green colonies (Fig. 2B), which occurred with a frequency of ~0.3% over total CFUs (for comparison, see Table T1). This value is exactly half that obtained by knocking-out single *CpFTSY* gene (~0.6%, see Table 1). This perfectly fits the expectation since only half the amount of RNPs transformed contained *CpFTSY* sgRNA, while the other half was composed of *PSR1* sgRNA. After pre-selection based on pale-green phenotype, colorimetric BCIP assay (Fig. 2C) identified double mutants *cpftsy psr1*, further confirmed by Sanger sequencing (Fig. 2F). We assessed the frequency of *PSR1* KOs in pale-green *cpftsy* mutants to about 22%. Indeed, out of the 9 confirmed pale-green colonies, 2 were co-edited by single nucleotide deletion; line A1 was both edited in T1 *PSR1* and T1 *CpFTSY*, while line A6 was both edited in T2 *PSR1* and T1 *CpFTSY*. By normalizing the number of double-edited colonies to the viable cells ($N_{viable\ cells}$, see Methods), a total number of 321±117 (n=6) pale-green colonies would have expected over the whole transformation sample (10^6 cells), resulting in a Y_{GE} of 3.21±1.17 ($\cdot 10^{-4}$) and 7.13±2.60 ($\cdot 10^{-5}$) for *CpFTSY* (single) and *CpFTSY PSR1* (double) editing, respectively (Table 4 S). It can be concluded that this DNA-free GE strategy is a reliable and efficient system for the simultaneous disruption of two target genes in *C. r.* Concerning the co-edited mutants, no events of dual cutting in the same locus, namely *PSR1* T1 and T2 or *CpFTSY* T1 and T2, were observed.

Summary of DNA-free GE efficiencies in *C. r.*

DNA-free GE efficiencies (Table 1) determined in this study were compared to the yield of a more conventional GE approach relying on introducing foreign DNA into cells and antibiotic selection [13]. The data is given as percentage frequency ($\%F_{GE}$) of pale-green colonies over total CFUs, and further related to the whole population transformed (10^6 cells), allowing us to compare Y_{GE} current values with that of the DNA-based approach. All relevant Cas9-induced mutations were verified by

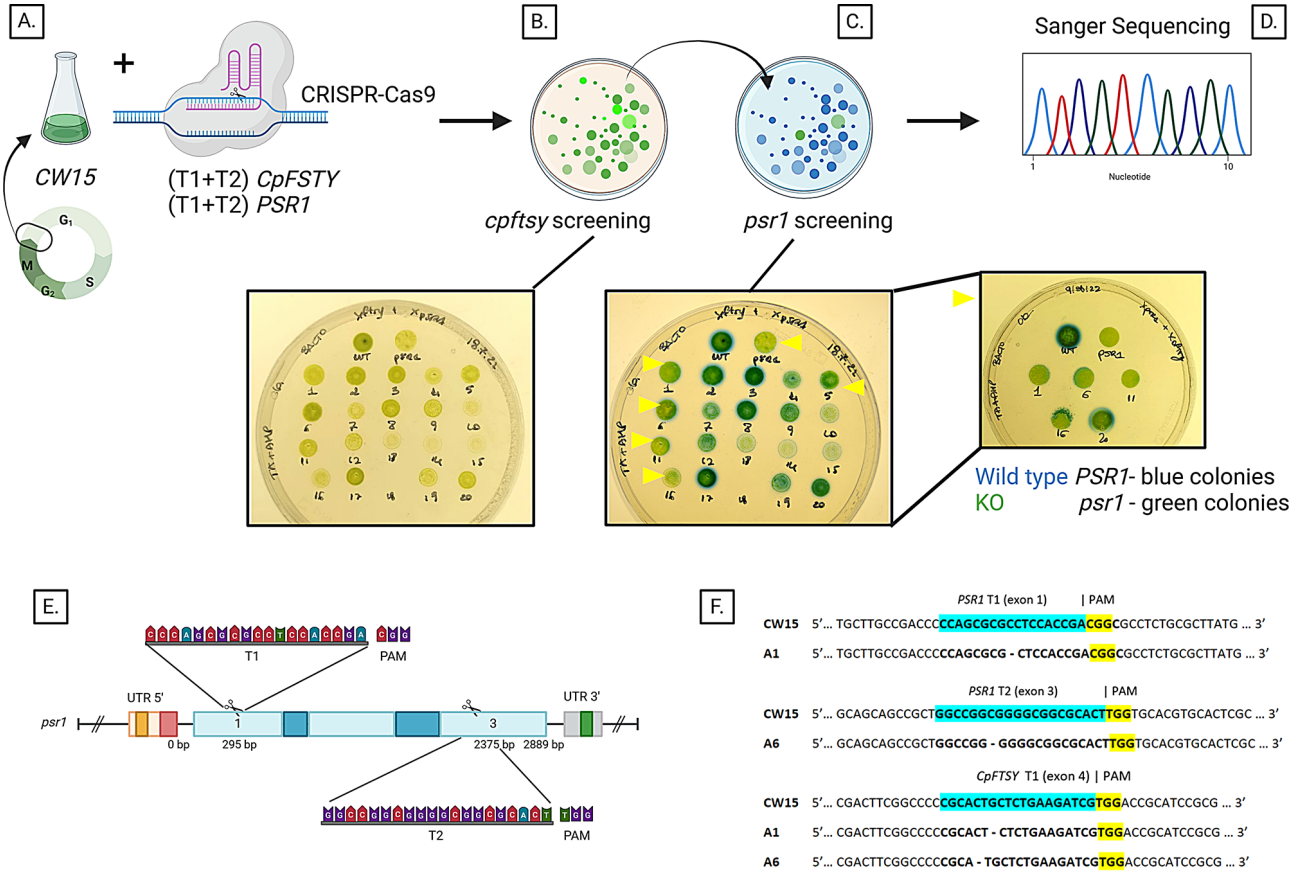

Fig. 2 DNA-free GE strategy co-targeting *cpftsy* and *psr1*. (**A**) CW15 synchronized cells were transformed by electroporation with RNPs of sgRNA guided to both the target sequences T1 and T2 of *CpFTSY* and target sequences T1 and T2 of *PSR1*. T1 and T2 of *PSR1* were chosen in exon 1 and 3, at position 295 bp and 1768 bp, respectively (Fig. 8S). (**B**) A first selection round was performed on TAP agar plates based on a pale-green phenotype. Selected colonies were streaked on new TAP agar plates to permit the isolation of single, genetically identical colonies. (**C**) A second screening was performed on TA agar plates devoid of phosphate and supplemented with BCIP, the latter used for the colorimetric detection of alkaline phosphatase activity. Colonies expressing PSR1 exhibited both blue and halo, while colonies devoid of functional PSR1 cannot process BCIP by PSR1-regulated phosphatases and resulted green. (**D**) Potential double mutants, highlighted with yellow arrows, were analyzed by Sanger sequencing of target regions of both *CpFTSY* (Fig. 1C) and *PSR1* (**E**). (**F**) Sequencing data output of *PSR1* and *CpFTSY* target regions T1 and T2, wild type sequences are highlighted in blue, and specific PAM motifs are in yellow. Missing nucleotides are indicated as "-" and nucleotide substitutions are highlighted in green. BCIP = 5-bromo-4-chloro-3-indolyl phosphate

sequencing the corresponding target sequence PCR amplicons (Fig. 3S S). Raw data from each single transformation event are also provided (Table 3S and 4 S).

(1st column) the growth conditions, either under optimal phosphate supplementation (+P) or phosphate starvation (-P); (2nd column) the transformation target(s) to knock-out (*CpFTSY* and/or *PSR1*); (3rd column) the total number of CFU (N_{CFU}) obtained upon 6 replicates; (4th column) the number of viable cells ($N_{viable\ cells}$), which was obtained multiplying the N_{CFU} by the factor of dilution plating (D); (5th column) the total number of pale-green colonies ($N_{pale-green\ colonies}$) over 6 replicates; (6th column) the GE frequency (F_{GE} %), namely $N_{pale-green\ colonies}$ over N_{CFU}; (7th column) the number of pale-green colonies which resulted from precise editing events (or co-edited) compared to $N_{pale-green\ colonies}$; (8th – 9th – 10th columns) the number of pale-green colonies which underwent an edit in either target T1, T2 or both, respectively; (11th column) the number of edited colonies normalized to D; (12th column) GE efficiency (Y_{GE}) calculated by the total number of edited colonies (11th column) and considering the whole cell population which underwent electroporation (10^6 cells); (13th column) the enhancement in GE efficiencies (folds) with respect to that reported [13] with antibiotic selection; (14th – 15th columns) frequency (%) of nucleotide insertion and/or deletion (±) or nucleotide substitution (⇄), respectively, in precisely edited lines. Each experiment was performed with 6 biological replicates ($n=6$), and 10 plates were used in each replicate. Statistical analysis of Y_{GE}: # p-value < 0.0001 for transformation without antibiotic selection vs. transformation with antibiotic gene integration [13]; § p-value = 0.1042 for (+P) vs. (-P) transformations. In bold text are highlighted the names of each factor under evaluation.

Discussion and outlook

In the presented study, we implemented an efficient DNA-free GE strategy in *C. r.* by exploiting different types of cell synchronization to achieve single targeting of *CpFTSY* and co-targeting of both *CpFTSY* and *PSR1*. In particular, we choose as main target the *CpFTSY* gene because (i) its disruption leads to an easy-to-detect pale-green phenotype due to a lower abundance of LHCs and, consequently, a significant reduction of chlorophyll content per cell [17, 20] and (ii) it was already used as target gene in other works [13, 16, 17] allowing to reduce the difference among the approaches and compare the results. We found that DNA integration event and functional expression of an antibiotic resistance marker are the major limiting steps in classical GE approaches in *C. r.*. Indeed, eliminating DNA integration enhanced the efficiency of single target gene disruption by more than 200-fold, with respect to previous reports [13] under conditions of light- and temperature-based cell synchronization.

In addition, in a recent approach, Freudenberg et al. in 2022 [24] investigated GE limiting factors based on cell synchronization, by forcing *C. r.* cells to enter and rest in the G_0 phase of the cell cycle through nitrogen starvation. This strategy increased the GE efficiency by 66% with respect to unsynchronized cells, thus approaching the GE enhancement upon culture synchronization by temperature and light [13]. Besides nitrogen, phosphorus (P), in the form of phosphate, is an essential macronutrient that promotes *C. r.* growth, playing an important role as a component of nucleic acids and providing energy for conducting metabolic processes. Therefore, based on the molecular implications of N starvation on the cell cycle, we hypothesized that extended application of P starvation might increase GE frequencies. To this aim, we induced P starvation on *C.r.* synchronized cell cultures. We could verify an increase in GE efficiency of more than 270-fold compared to the DNA-based approach [13] and 34.5% higher than DNA-free GE under optimal P supplementation (shown in this study).

Interestingly, the enhancement of GE efficiency upon P starvation of pre-cultures was in agreement with recent results by Freudenberg and coworkers [24] under nitrogen starvation conditions. This also expands the opportunities for DNA-free GE applications, which specific starvation conditions might further enhance. It is worth noting that the increase in Y_{GE} is significantly different ($p^{**} < 0.0001$) concerning more conventional GE approaches (see Table 1) which rely on DNA integration [13], but only slightly higher ($p^{*} = 0{,}1042$) with respect to antibiotic-free (-AB) GE based on light- and temperature-induced cell synchronization (data here reported).

Therefore, this finding constitutes a valuable extension to the collection of treatments implemented for precise gene editing in *C. r.*, which makes possible the prospective choice of specific pre-culture conditions dependent on desired gene disruption strategies.

We could speculate that the advantage of nutrient starvation ([13, 31], current report) over modulation of light and temperature conditions [13, 31] in enhancing Y_{GE} might be ascribed to a more efficient cell synchronization in the former. Alternatively, the effect of nutrient starvation is the arrest of the cell cycle at the G_0 phase, in which DNA replication is prevented [32]. This could provide an extended time frame for Cas9 to introduce DNA DSBs on relaxed chromatin structure, thus increasing the frequency of NHEJ-mediated repair. The latter appears to be complexly regulated in eukaryotes upon different types of DSBs, especially the so-called DSBs with chromatin- or end-complexity (e.g. after Cas9-mediated DSB introduction), which require a slower kind of NHEJ mediated repair (as reviewed for eukaryotes in [33]) and thus might benefit from prolonged time for repair during cell arrest. Moreover, the Y_{GE} of specific genes might be highly variable, as previously indicated [20], depending on various factors such as nuclease accessibility given by chromatin structure or disturbing presence of DNA-binding proteins as well as different efficiency of sgRNA annealing to the target [34]. Although again speculative, findings from other eukaryotes may indicate that transcriptionally active DNA sites are highly susceptible to DNA damage with a fast DNA repair response [35] and thus might be more efficiently targeted in gene disruption approaches compared to transcriptionally inactive DNA sites.

We developed a co-editing DNA-free tool to test our strategy on genes lacking an easy-to-detect phenotype further. Indeed, mutants without an easily detectable phenotype are often generated through pre-selection using an antibiotic resistance marker [6, 15, 18, 20]. Nonetheless, co-selection via mutation of an endogenous gene producing a selectable phenotype has been recently reported [16, 36], although this approach still needs to improve for low efficiency. The possibility of targeting multiple independent loci was hypothesized based on several assumptions, namely (i) the successful uptake of different RNPs into the cell and (ii) the stability of RNPs in the nucleus, which should be retained long enough to introduce more than one DSB with subsequent NHEJ mediated DSB repair and thus enabling multiple targeting. Hence, we efficiently edited the *PSR1* locus with a co-targeting frequency of 22% and hereby paved the way for future advancement in DNA-free multiple gene editing. Interestingly, close target regions within each gene were discriminated for dual targeting compared to distant target regions, as shown for both *CpFTSY* (chromosome 5) and *PSR1* (chromosome 12): the efficiency for T1 and T2 dual disruption was, on average, around 0.1%. This evidence alows for the hypothesis that induction of

a DSB by Cas9 and subsequent NHEJ-based repair of the target site resulted in the surrounding DNA molecule being occupied by sequential assembly of repair factors [37], thus inhibiting the accessibility of Cas9 to other close target regions. Moreover, it was reported that Cas9 proteins stably bind to the target site for several hours [38], thereby inhibiting other Cas9 complexes from acting on close domains. Considering these hypotheses, future work could assess a minimal distance between target regions, ensuring efficient dual disruption.

Interestingly, the error-prone DNA repair mechanism by NHEJ accounted for the mutations induced, mainly resulting in the deletion of single nucleotides causing frameshifts (76–82%), thus impairing protein function [17]. Moreover, the current strategy avoided the use of DNA for targeted gene disruption and thereby overcame random insertion of DNA molecules into the genome, these events potentially leading to unpredictable and undesired effects. However, innovative DNA-based GE approaches have been reported, such as using single-stranded oligodeoxynucleotides (ssODNs) for targeted gene disruption and selectable marker production [16]. These strategies advanced precise gene editing in *C. r.*, though future work should focus on avoiding random DNA insertion.

The transgene-free GE strategy investigated here opens new perspectives for generating complex genotypes, providing a straightforward routine for functional analysis of complex pathways or gene families in *C. r.* Moreover, the high GE frequency here shown by specific pre-culture treatments, provides new prospectives and potential applications for multiple gene targeting in microalgal species of industrial interest. Higher-order mutants could be generated through subsequent transformations, even though the approach still depends on easy-to-detect phenotypes. Additional applications include exploiting sequence homologies between genes, simultaneously targeting multiple independent loci by multiplexing and unraveling overlapping or redundant functions. Further improvement of DNA-free GE applications in *C. r.* could focus on the optimization of the transformation procedure itself, i.e. either by enhancing RNP delivery into the cell, or by assessing optimal sgRNA: Cas9 stoichiometry [13, 17], or through enhancing sgRNA target binding efficiencies. Other specific nucleases, such as Cas12a [39] could also be tested to identify the best candidates for efficient DNA-free editing.

Supplementary Information

The online version contains supplementary material available at https://doi.org/10.1186/s13062-024-00545-3.

Supplementary Material 1

Acknowledgements
The authors would like to thank Claudia Buechel for her helpful discussion.

Author contributions
R.B. and M.A. initiated the project; C.B. planned and conducted the experiments supported by M.A.; C.B., M.A., L.D.O. and R.B wrote the manuscript.

Funding
The authors acknowledge the financial support from the Ministry of Education, University and Research (MIUR grant driveALGAE – 2022FXRZBF - PRIN2022) to LD, and from the European Research Council (ERC Advanced Grant 101053983-GrInSun) to RB.

Data availability
No datasets were generated or analysed during the current study.

Declarations

Ethics approval and consent to participate
Not applicable.

Competing interests
The authors declare no competing interests.

Received: 27 September 2024 / Accepted: 8 October 2024
Published online: 11 November 2024

References

1. Cutolo EA, Caferri R, Guardini Z, Dall'Osto L, Bassi R. Analysis of state 1—state 2 transitions by genome editing and complementation reveals a quenching component independent from the formation of PSI-LHCI-LHCII supercomplex in Arabidopsis thaliana. Biol Direct. 2023;18.
2. Einhaus A, Steube J, Freudenberg RA, Barczyk J, Baier T, Kruse O. Engineering a powerful green cell factory for robust photoautotrophic diterpenoid production. Metab Eng. 2022;73:82–90.
3. Scaife MA, Nguyen GTDT, Rico J, Lambert D, Helliwell KE, Smith AG. Establishing Chlamydomonas reinhardtii as an industrial biotechnology host. Plant J. 2015;82:532–46.
4. Zhang YT, Jiang JY, Shi TQ, Sun XM, Zhao QY, Huang H et al. Application of the CRISPR/Cas system for genome editing in microalgae. Appl Microbiol Biotechnol. Springer Verlag; 2019.
5. Jinkerson RE, Jonikas MC. Molecular techniques to interrogate and edit the Chlamydomonas nuclear genome. Plant J. 2015;82:393–412.
6. Picariello T, Hou Y, Kubo T, McNeill NA, Yanagisawa HA, Oda T et al. TIM, a targeted insertional mutagenesis method utilizing CRISPR/Cas9 in Chlamydomonas reinhardtii. PLoS ONE. 2020;15.
7. Jiang W, Brueggeman AJ, Horken KM, Plucinak TM, Weeks DP. Successful transient expression of Cas9 and single guide RNA genes in Chlamydomonas reinhardtii. Eukaryot Cell. 2014;13:1465–9.
8. González Castro N, Bjelic J, Malhotra G, Huang C, Alsaffar SH. Comparison of the feasibility, efficiency, and safety of genome editing technologies. Int J Mol Sci MDPI. 2021;22:10355. https://doi.org/10.3390/ijms221910355.
9. Li JF, Norville JE, Aach J, McCormack M, Zhang D, Bush J, et al. Multiplex and homologous recombination-mediated genome editing in Arabidopsis and Nicotiana benthamiana using guide RNA and Cas9. Nat Biotechnol. 2013;31(8):688–91. https://doi.org/10.1038/nbt.2654. PMID: 23929339; PMCID: PMC4078740.
10. Wang H, Yang H, Shivalila CS, Dawlaty MM, Cheng AW, Zhang F, et al. One-step generation of mice carrying mutations in multiple genes by CRISPR/Cas-mediated genome engineering. Cell. 2013;153:910–8.
11. Doudna JA, Charpentier E. The new frontier of genome engineering with CRISPR-Cas9 [Internet]. https://www.science.org
12. Boel A, De Saffel H, Steyaert W, Callewaert B, De Paepe A, Coucke PJ et al. CRISPR/Cas9-mediated homology-directed repair by ssODNs in zebrafish induces complex mutational patterns resulting from genomic integration of repair-template fragments. DMM Disease Models Mech. 2018;11.
13. Angstenberger M, De Signori F, Vecchi V, Dall'Osto L, Bassi R. Cell synchronization enhances Nuclear Transformation and Genome Editing via Cas9

enabling homologous recombination in Chlamydomonas reinhardtii. ACS Synth Biol. 2020;9:2840–50.
14. Guzmán-Zapata D, Sandoval-Vargas JM, Macedo-Osorio KS, Salgado-Manjarrez E, Castrejón-Flores JL, Oliver-Salvador MDC, et al. Efficient editing of the nuclear APT reporter gene in chlamydomonas reinhardtii via expression of a CRISPR-Cas9 module. Int J Mol Sci. 2019;20(5):1247. https://doi.org/10.3390/ijms20051247. PMID: 30871076; PMCID: PMC6429146.
15. Greiner A, Kelterborn S, Evers H, Kreimer G, Sizova I, Hegemann P. Targeting of photoreceptor genes in Chlamydomonas reinhardtii via zinc-finger nucleases and CRISPR/Cas9. Plant Cell. 2017;29:2498–518.
16. Akella S, Ma X, Bacova R, Harmer ZP, Kolackova M, Wen X, et al. Co-targeting strategy for precise, scarless gene editing with CRISPR/Cas9 and donor ssODNs in Chlamydomonas. Plant Physiol. 2021;187:2637–55.
17. Baek K, Kim DH, Jeong J, Sim SJ, Melis A, Kim JS et al. DNA-free two-gene knockout in Chlamydomonas reinhardtii via CRISPR-Cas9 ribonucleoproteins. Sci Rep. 2016;6.
18. Shin SE, Lim JM, Koh HG, Kim EK, Kang NK, Jeon S et al. CRISPR/Cas9-induced knockout and knock-in mutations in Chlamydomonas reinhardtii. Sci Rep. 2016;6.
19. Ferenczi A, Pyott DE, Xipnitou A, Molnar A, Merchant SS. Efficient targeted DNA editing and replacement in Chlamydomonas reinhardtii using Cpf1 ribonucleoproteins and single-stranded DNA. Proc Natl Acad Sci U S A. 2017;114:13567–72.
20. Kim J, Lee S, Baek K, Jin ES. Site-Specific Gene knock-out and On-Site heterologous gene overexpression in Chlamydomonas reinhardtii via a CRISPR-Cas9-Mediated knock-in method. Front Plant Sci. 2020;11.
21. Kang S, Jeon S, Kim S, Chang YK, Kim YC. Development of a pVEC peptide-based ribonucleoprotein (RNP) delivery system for genome editing using CRISPR/Cas9 in Chlamydomonas reinhardtii. Sci Rep. 2020;10.
22. Bloomer H, Khirallah J, Li Y, Xu Q. CRISPR/Cas9 ribonucleoprotein-mediated genome and epigenome editing in mammalian cells. Adv Drug Deliv Rev. Elsevier B.V.; 2022.
23. Lattanzi A, Meneghini V, Pavani G, Amor F, Ramadier S, Felix T, et al. Optimization of CRISPR/Cas9 delivery to human hematopoietic stem and progenitor cells for therapeutic genomic rearrangements. Mol Ther. 2019;27:137–50.
24. Freudenberg RA, Wittemeier L, Einhaus A, Baier T, Kruse O. The Spermidine synthase gene SPD1: a novel auxotrophic marker for Chlamydomonas reinhardtii designed by enhanced CRISPR/Cas9 gene editing. Cells. 2022;11.
25. Ghribi M, Nouemssi SB, Meddeb-Mouelhi F, Desgagné-Penix I. Genome editing by CRISPR-Cas: a game change in the genetic manipulation of chlamydomonas. Life. MDPI AG; 2020. pp. 1–21.
26. Shamoto N, Narita K, Kubo T, Oda T, Takeda S. CFAP70 is a novel axoneme-binding protein that localizes at the base of the outer dynein arm and regulates ciliary motility. Cells. 2018;7.
27. Grossman AR, Usuda H, Shimogawara K. A nuclear localized protein that regu-lates phosphorus metabolism in Chlamydomonas [Internet]. 1999. https://www.researchgate.net/publication/244973054
28. Kropat J, Hong-Hermesdorf A, Casero D, Ent P, Castruita M, Pellegrini M, et al. A revised mineral nutrient supplement increases biomass and growth rate in Chlamydomonas reinhardtii. Plant J. 2011;66:770–80.
29. Kira N, Ohnishi K, Miyagawa-Yamaguchi A, Kadono T, Adachi M. Nuclear transformation of the diatom Phaeodactylum tricornutum using PCR-amplified DNA fragments by microparticle bombardment. Mar Genomics. 2016;25:49–56.
30. Formighieri C, Franck F, Bassi R. Regulation of the pigment optical density of an algal cell: filling the gap between photosynthetic productivity in the laboratory and in mass culture. J Biotechnol. 2012;162:115–23.
31. Strenkert D, Schmollinger S, Gallaher SD, Salomé PA, Purvine SO, Nicora CD, et al. Multiomics resolution of molecular events during a day in the life of Chlamydomonas. Proc Natl Acad Sci U S A. 2019;116:2374–83.
32. Zachleder V, Ivanov I, Vítová M, Bišová K. Cell cycle arrest by supraoptimal temperature in the alga Chlamydomonas reinhardtii. Cells. 2019;8.
33. Shibata A, Jeggo A. AdvAnces in rAdiAtion biology-HigHligHts from 16 tH icrr speciAl feAture: review Article canonical dnA non-homologous end-joining; capacity versus fidelity. 2020.
34. Xu H, Xiao T, Chen CH, Li W, Meyer CA, Wu Q, et al. Sequence determinants of improved CRISPR sgRNA design. Genome Res. 2015;25:1147–57.
35. Marnef A, Cohen S, Legube G, Transcription-Coupled DNA. Double-Strand Break Repair: Active Genes Need Special Care. J Mol Biol. Academic Press; 2017. pp. 1277–88.
36. Xue JH, Chen GD, Hao F, Chen H, Fang Z, Chen FF, et al. A vitamin-C-derived DNA modification catalysed by an algal TET homologue. Nature. 2019;569:581–5.
37. Vogt A, He Y. Structure and mechanism in non-homologous end joining. DNA Repair (Amst). 2023;130.
38. Richardson CD, Ray GJ, DeWitt MA, Curie GL, Corn JE. Enhancing homology-directed genome editing by catalytically active and inactive CRISPR-Cas9 using asymmetric donor DNA. Nat Biotechnol. 2016;34:339–44.
39. Schindele P, Puchta H. Engineering CRISPR/LbCas12a for highly efficient, temperature-tolerant plant gene editing. Plant Biotechnol J. 2020;18:1118–20.

Publisher's note